

Lead Sorption on Ruthenium Oxide: A Macroscopic and Spectroscopic Study

K.G. Scheckel, C.A. Impellitteri, J.A. Ryan

National Risk Management Research Laboratory, U.S. Environmental Protection Agency (EPA),
Cincinnati, OH, U.S.A.

Introduction

Metal oxide phases play an important role in governing the sorption and desorption mechanisms of metals in water, soils, and sediments. Many researchers have examined the efficiency of Pb sorption on Mn, Fe, Al, Ti, and Si oxide surfaces. Most studies concluded that adsorption of Pb onto the oxide surface was the sorption mechanism. Some studies, however, observed induced coprecipitation of Pb with the oxide phase. To ensure that the remediation sorbent for removing Pb from solution, is effective, a cost analysis of the amount of Pb sorbed per unit cost of sorbent must be done. Most of the examples listed above rarely achieve more than a few weight percent Pb sorbed per unit weight of sorbent. Beyond the ability to sorb large amounts of Pb from solution, understanding the sorption mechanism and potential stability of the Pb complex yields data applicable for designing higher-capacity and more-efficient sorbents.

In this study, the sorption of Pb on $\text{RuO}_2 \cdot x\text{H}_2\text{O}$ was examined kinetically and thermodynamically via spectroscopic and macroscopic investigations. X-ray absorption spectroscopy (XAS) was employed to determine the sorption mechanism with regard to the identity of the nearest atomic neighbors, bond distances (R), and coordination numbers (N). Impellitteri et al. [1] recently examined the effectiveness of RuO_2 in removing arsenate and arsenite from solution (pH 7), with equilibrium surface loadings approaching 10% and 20% wt/wt, respectively. We designed experiments to investigate the sorption of Pb on RuO_2 via spectroscopic and macroscopic methods to elucidate the sorption mechanism, sorption capacity, and Pb retention.

Methods and Materials

To investigate the influence of time on Pb sorption, pH-stat kinetic experiments were conducted for $\text{RuO}_2 \cdot x\text{H}_2\text{O}$ reacted with Pb at pH 6. In a 1-L Teflon[®] reaction vessel, 5 g of $\text{RuO}_2 \cdot x\text{H}_2\text{O}$ was reacted with 500 mL of combined background electrolyte and appropriate stock solution to obtain initial Pb concentrations of 207.2, 2072, and 10, 360 mg/L. Kinetic samples were collected at time 0 through approximately 40 h at which time the reaction appeared to be complete.

For the equilibrium studies, initial concentrations of Pb were increased in 100-mg/L increments from 0 to 1000 mg/L and in 500-mg/L increments from 1000 to 2000 mg/L. The suspensions were placed on an end-over-end shaker at 30 rpm, and the pH's (target pH = 6) of the samples were adjusted 3-5 times daily under N_2 purge. The pH was adjusted to pH 6 via inputs of either NaOH or HNO_3 until the pH stabilized.

Pb-reacted $\text{RuO}_2 \cdot x\text{H}_2\text{O}$ kinetic samples were analyzed by x-ray absorption near-edge spectroscopy (XANES) and x-ray absorption fine structure (XAFS) spectroscopy to determine Pb speciation and related local atomic parameters for Pb on the surface of $\text{RuO}_2 \cdot x\text{H}_2\text{O}$. For XANES and XAFS studies, a thin layer of a Pb-reacted $\text{RuO}_2 \cdot x\text{H}_2\text{O}$ sample was smeared onto Kapton[®] tape and folded back on itself. Pb (13055 eV) LIII-XANES and XAFS data were collected at PNC-CAT beamline 20-BM at the APS. The electron storage ring operated at 7 GeV. Three to five scans were collected at ambient temperature in transmission mode. XANES and XAFS spectra were collected in both transmission and fluorescence modes with a solid-state 13-element detector. Reference samples of $\text{Pb}_4\text{OH}_4^{4+}$ and $\text{Pb}(\text{NO}_3)_2$ were collected for comparison with the XANES spectra. The collected scans for a particular sample were averaged, the data were then normalized, and the background was removed by spline fitting by using WinXAS 2.0. The XAFS data were then converted to k -space, windowed, and Fourier transformed to convert to R -space. Conventional shell-by-shell fitting of the radial structure functions (RSFs) was attempted by theoretical paths for Pb and O backscatter atoms generated from crystallographic data of model compounds by using FEFF 7.0. Variables obtained from the fits included the energy phase shift (ΔE_0), coordination numbers (N), bond distances (R), and Debye-Waller factors (σ^2) that were derived from nonlinear least squares fitting.

Results and Discussion

Figure 1 shows the kinetic uptake of Pb from solution for initial Pb concentrations of 207.2, 2072, and 10, 360 mg/L in a 10-g $\text{RuO}_2 \cdot x\text{H}_2\text{O}$ /1-L suspension. For the lower initial Pb concentrations of 207.2 and 2072 mg/L, nearly complete sorption was observed within 5 min of the reaction time for sorption

weight percents of about 2% and 20%, respectively. It was not until we attempted an extremely high initial Pb concentration of 10, 360 mg/L under controlled conditions that a measured maximum sorption capacity of approximately 95% wt/wt of Pb on the $\text{RuO}_2 \cdot x\text{H}_2\text{O}$ surface through the 42-h reaction time was obtained. These results demonstrate that Pb sorption on $\text{RuO}_2 \cdot x\text{H}_2\text{O}$ is very rapid, with an enormously high capacity.

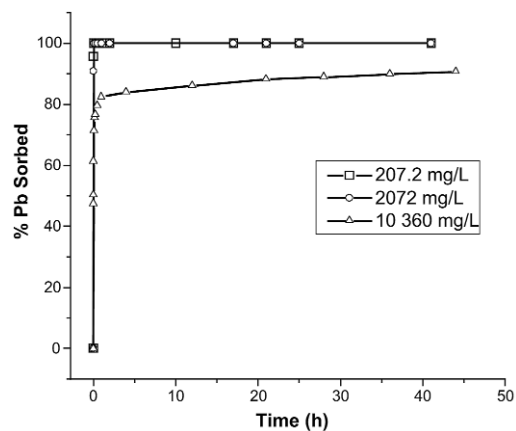


FIG. 1. Kinetics of Pb sorption on $\text{RuO}_2 \cdot x\text{H}_2\text{O}$ as a function of Pb concentration at pH 6.

The equilibrium sorption results at pH 6 for Pb- $\text{RuO}_2 \cdot x\text{H}_2\text{O}$ are shown in Fig. 2. The initial Pb concentration for the samples ranged from 0 to 2000 mg/L for the 1-g $\text{RuO}_2 \cdot x\text{H}_2\text{O}$ /1-L solution. For nearly all samples, except the three highest Pb concentrations of 1000, 1500, and 2000 mg/L, no detectable Pb remained in solution at equilibrium after 5 d of reaction. Notice there is no sharp upward tailing at the higher

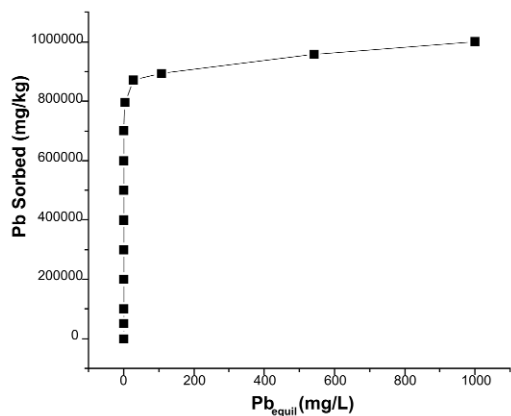


FIG. 2. Thermodynamic equilibrium study of Pb sorption on $\text{RuO}_2 \cdot x\text{H}_2\text{O}$ as a function of Pb concentration at pH 6.

concentrations that could be indicative of surface precipitation; however, assigning a sorption mechanism based on the shape of an adsorption curve should be avoided [2]. These data were plotted against the Langmuir and Freundlich adsorption models. The Langmuir parameters suggest a maximum monolayer sorption level b to be 9.92×10^5 mg/kg, which is very close to our measured value of approximately 1.00×10^6 mg/kg. The binding strength constant k is 4.65×10^{11} , suggesting a strong binding potential. The Freundlich model predicts a distribution coefficient K_d of 3.45×10^{13} . A correction factor n of 25.9 ($1/n = 0.0386$) indicates the nonlinearity of the data.

The sensitive first-shell coordination environment of Pb L_{III}-XANES spectra is shown in Fig. 3. XANES spectra can be used to infer the molecular structure of the Pb sorption complexes on the $\text{RuO}_2 \cdot x\text{H}_2\text{O}$ surface through comparison with reference compounds with known coordination environments on the basis of differences in the degree of distortion and the number of nearest neighbor O atoms for a given Pb coordination sphere. Shown in Fig. 3 are reference compounds of $\text{Pb}(\text{NO}_3)_2$ (stock solution material) and $\text{Pb}_4\text{OH}_4^{4+}$ (prepared according to Ref. 3) relative to the kinetics

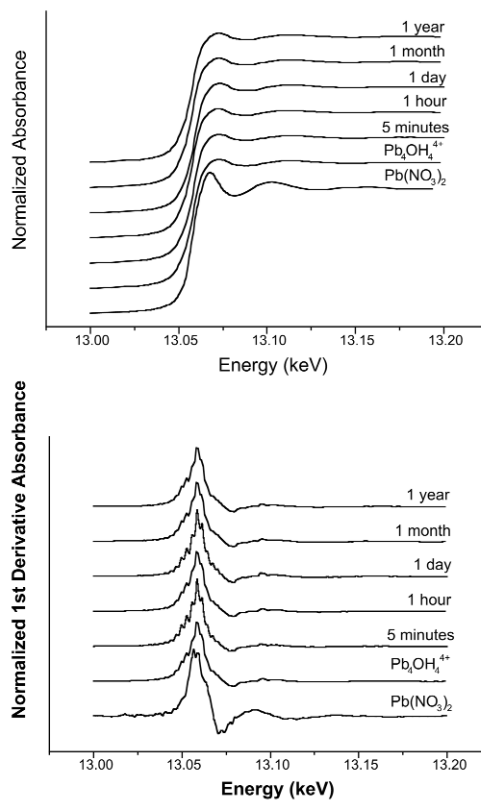


FIG. 3. Normalized XANES spectra and first derivatives of XANES spectra from Pb-reacted $\text{RuO}_2 \cdot x\text{H}_2\text{O}$ aged samples and reference samples.

samples of Pb sorption on $\text{RuO}_2 \cdot x\text{H}_2\text{O}$. The Pb- $\text{RuO}_2 \cdot x\text{H}_2\text{O}$ sorption sample spectra are essentially identical to the $\text{Pb}_4\text{OH}_4^{4+}$ XANES curve, indicating that the first-shell coordination environment of Pb is present as distorted trigonal pyramids in the sorption samples, which is indicative of inner-sphere adsorption complexes. Derivatives of the XANES spectra show in more detail the sensitive first-shell coordination environment (Fig. 3). Relative to the Pb-sorbed $\text{RuO}_2 \cdot x\text{H}_2\text{O}$ samples, the $\text{Pb}_4\text{OH}_4^{4+}$ spectrum is very similar to the sorption samples, reinforcing the theory of distorted trigonal pyramids with high covalency of Pb in the samples as a result of a stereoactive lone pair of electrons yielding strongly asymmetric coordination polyhedra (OH^- ligands) about the Pb cation. The close proximity of these complexes in this coordination is favorable for formation of Pb-Pb dimers [4].

Chi function (k^3 -weighted) spectra of the extended x-ray absorption fine structure (EXAFS) spectroscopy

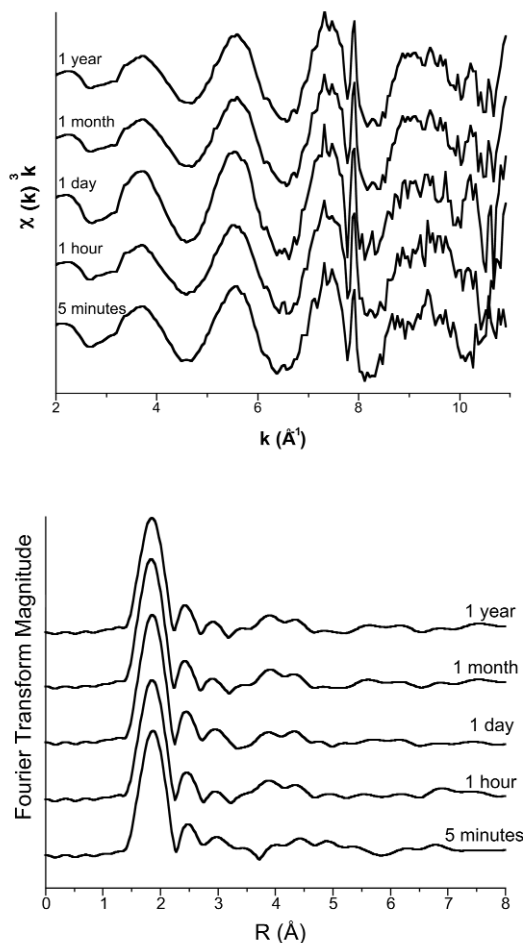


FIG. 4. The k^3 -weighted χ functions and Fourier transformed radial structure functions of Pb-reacted $\text{RuO}_2 \cdot x\text{H}_2\text{O}$ samples aged from 5 min to 1 yr.

data are presented in Fig. 4 for the Pb- $\text{RuO}_2 \cdot x\text{H}_2\text{O}$ sorption samples. The χ structures show no changes as the reaction time increases from 5 min to 1 yr and resemble the χ function of $\text{Pb}_4\text{OH}_4^{4+}$ (data not shown). An interesting beat pattern observed at approximately 7.9 \AA^{-1} shows a distinct independent peak associated with a broader peak within the χ function. No obvious glitches in the raw data were noticed to give rise to such a structure. The authors theorize that it may be the result of the unique ruthenium oxide surface influencing the reaction with Pb. To gain a better insight into the oscillations evident in the χ structures, the k^3 -weighted spectra were Fourier transformed into radial structure functions (RSFs).

The EXAFS fitting results of the RSFs for Pb sorption on $\text{RuO}_2 \cdot x\text{H}_2\text{O}$ indicate that the Pb adsorbed as polynuclear bidentate inner-sphere Pb-Pb dimer complexes with first-shell Pb-O parameters of $R_{\text{Pb-O}} = 2.27 \text{ \AA}$ and $N_{\text{Pb-O}} = 2.1-2.5$. Pb-Ru interatomic associations suggest two distinct surface coordinations of Pb to edges ($R_{\text{Pb-Ru}_I}$ of $\sim 3.38 \text{ \AA}$ and $N_{\text{Pb-Ru}_I}$ of ~ 1.0) and shared corners ($R_{\text{Pb-Ru}_{II}}$ of $\sim 4.19 \text{ \AA}$ and $N_{\text{Pb-Ru}_{II}}$ of ~ 0.8) on the RuO_2 octahedra. Because of the high sorption coverage of Pb, the formations of Pb-Pb dimers ($R_{\text{Pb-Pb}}$ of $\sim 3.89 \text{ \AA}$ and $N_{\text{Pb-Pb}}$ of ~ 0.9) were also distinguishable in the second shell. While the XANES data (Fig. 3) indicate that the Pb sorption complex is similar to $\text{Pb}_4\text{OH}_4^{4+}$ coordination (distorted trigonal pyramids), the XANES spectra cannot predict the interaction of neighboring sorption complexes to form Pb-Pb dimers. The kinetic data for these samples show that for the first XAFS sample (reaction time = 5 min), more than 50% of the initial Pb in solution is sorbed to the ruthenium oxide surface, for an approximate surface coverage of 50% wt/wt. The Pb-Pb interaction in the second shell cannot be described by the formation of Pb precipitate phases on the basis of a comparison of unpublished XAFS data on Pb hydroxides and oxides made by the authors. The high surface concentration of Pb, coupled with the rapid kinetics, explains the observed Pb-Pb dimers within 5 min of reaction.

Acknowledgments

PNC-CAT facilities and research at these facilities is supported by U.S. Department of Energy (DOE) Office of Science Grant No. DE-FG03-97ER45628. Use of the APS was supported by the DOE Office of Science, Office of Basic Energy Sciences, under Contract No. W-31-109-ENG-38. The authors extend their deepest appreciation to the staff of the PNC-CAT, especially beamline scientist R. Gordon for his assistance and expertise during data collection. The EPA has not subjected this manuscript to internal policy review. Therefore, the research results presented herein do not, necessarily, reflect Agency policy. Mention of trade

names of commercial products and companies does not constitute endorsement or recommendation for use. Existing data not generated by EPA employees for informational purposes were not subjected to EPA's quality assurance procedures and there was no attempt to verify the quality of the data collected from the various sources.

References

- [1] C.A. Impellitteri, K.G. Scheckel, and J.A. Ryan, *Environ. Sci. Technol.* **37**, 2936-2940 (2003).
- [2] D.L. Sparks, *Environmental Soil Chemistry* (Academic Press, Inc., San Diego, CA, 1995).
- [3] D.G. Strawn and D.L. Sparks, *J. Colloid Interface Sci.* **216**, 257-269 (1999).
- [4] J.R. Bargar, G.E. Brown, Jr., and G.A. Parks, *Geochim. Cosmochim. Acta* **61**, 2617-2637 (1997).